Available on line at
Association of the Chemical Engineers of Serbia *AChE*
www.ache.org.rs/CICEQ
Chemical Industry & Chemical Engineering Quarterly 18 (2) 305–314 (2012)
CI&CEQ

R. MUTHURAJ[1]
S. SRINIVAS[2]
D. LOURDU IMMACULATE[3]

[1]Department of Mathematics, P.S.N.A. College of Eng. &Tech., Dindigul, India
[2]Fluid Dynamics Division, VIT University, Vellore, India
[3]Department of School education, Othakadi, Madurai, Government of Tamilnadu, India

SCIENTIFIC PAPER

UDC 519.87:532.57:66

DOI 10.2298/CICEQ111122007M

COMBINED EFFECTS OF CHEMICAL REACTION AND TEMPERATURE DEPENDENT HEAT SOURCE ON MHD MIXED CONVECTIVE FLOW OF A COUPLE-STRESS FLUID IN A VERTICAL WAVY POROUS SPACE WITH TRAVELLING THERMAL WAVES

A mathematical model is developed to examine the effect of chemical reaction on MHD mixed convective heat and mass transfer flow of a couple-stress fluid in vertical porous space in the presence of a temperature dependent heat source with travelling thermal waves. The dimensionless governing equations are assumed to be made up of two parts: a mean part corresponding to the fully developed mean flow, and a small perturbed part, using amplitude as a small parameter. The analytical solution of the perturbed part has been carried out using the long-wave approximation. The expressions for the zeroth order and the first order solutions are obtained and the results of the heat and mass transfer characteristics are presented graphically for various values of parameters entering into the problem. It is noted that velocity of the fluid increases with the increase of the couple stress parameter and increasing the chemical reaction parameter leads suppress the velocity of the fluid. Cross velocity decreases with an increase of the phase angle. The increase of the chemical reaction parameter and Schmidt number lead to decrease the fluid concentration. The hydrodynamic case for a non-porous space in the absence of the temperature dependent heat source for Newtonian fluid can be captured as a limiting case of our analysis by taking $H, \alpha_1 \to 0$, $D_a \to \infty$ *and* $a \to \infty$.

Keywords: mixed convection, wavy walls, porous space, couple-stress fluid and chemical reaction.

Mixed convection flow in a vertical channel has attracted much attention because of its practical applications. These include cooling of electronic equipment, heat exchangers, chemical processing equipments, gas-cooled nuclear reactors and others. Tao [1] studied the laminar, fully developed mixed convection in a vertical channel with uniform wall temperatures. Later, Aung and Worku [2] discussed the theory of combined free and forced convection in a vertical channel with flow reversal conditions for both developing and fully developed flows. Due to its widespread applications, several authors have studied the work on mixed convection [3-9]. Eldabe *et al.* [7] discussed the problem of mixed convective heat and mass transfer in a non-Newtonian fluid at a peristaltic surface with temperature dependent viscosity. Srinivas and Muthuraj [8] have discussed the effects of thermal radiation and space porosity on MHD mixed convection flow in a vertical channel using homotopy analysis method. Also, they have reported the problem of mixed convective heat and mass transfer in a vertical wavy channel through porous medium with travelling thermal waves [9]. Zheng *et al.* [10] have examined the unsteady flow and heat transfer on a permeable stretching sheet in the presence of non-uniform heat source/sink. Kumar *et al.* [11] have discussed the mixed convective flow and heat transfer in a vertical channel with one region filled with conducting fluid and another region with non-conducting fluid.

Correspondening author: S. Srinivas, Fluid Dynamics Division, VIT University, Vellore – 632 014, India.
E-mail: srinusuripeddi@hotmail.com
Paper received: 22 November, 2011
Paper revised: 18 January, 2012
Paper accepted: 21 January, 2012

The study of couple-stress fluids has applications in a number of processes that occur in industry such as the extrusion of polymer fluids, solidification of liquid crystals, cooling of metallic plate in a bath, exotic lubricants, and colloidal solutions, etc. The constitutive equations for couple-stress fluids are given by Stokes [12]. The theory proposed by Stokes is the simplest one for micro-fluids, which allows polar effects such as the presence of couple-stress, body couple, and non-symmetric tensors. Various studies on couple stress fluid have been made under different physical aspects. However, some recent contributions in the field may be mentioned in Refs. [12-21]. Mekheimer [17] analyzed the MHD flow of a conducting couple stress fluid in a slit channel with rhythmically contracting walls. Sobh [18] studied the effect of slip velocity on peristaltic flow of a couple-stress fluid in uniform and non-uniform symmetric channels using long wavelength approximation. Srinivasacharya *et al.* [19] have reported the incompressible laminar flow of a couplestress fluid in a porous channel with expanding or contracting walls using similarity transformation. Pandey and Chaube [20] have studied the wall properties on peristaltic transport of a couple-stress fluid using perturbation technique. More recently, Nadeem and Akram [21] have examined the peristaltic transport of a couplestress fluid in an asymmetric channel with the effect of the induced magnetic field under the assumptions of long wave length and low but finite Reynolds number.

Mixed convection flows with simultaneous heat and mass transfer under the influence of a magnetic field and chemical reaction arise in many transport processes both naturally and in many branches of science and engineering applications. Some recent interesting contributions on this topic can be found in the studies [22-27]. Pal and Talukdar [26] have analyzed the unsteady magnetohydrodynamic convective heat and mass transfer in a boundary layer slip flow past a vertical permeable plate with thermal radiation and chemical reaction using perturbation technique. Hayat *et al.* [27] have described the unsteady flow with heat and mass transfer characteristics in a third grade fluid bounded by a stretching sheet. Most recently, Srinivas and Muthuraj [28] have examined the effects of chemical reaction and space porosity on MHD mixed convective flow in a vertical asymmetric channel with peristalsis. They considered the flow is examined in a wave frame of reference moving with the velocity of the wave. The channel asymmetry is produced by choosing the peristaltic wave train on the walls to have different amplitude and phase. To the best of our knowledge, no investigation has been made to analyze the heat and mass transfer effects on MHD flow of couple stress fluid in a vertical channel with chemical reaction. Keeping this in view and motivated by the earlier studies, an attempt has been made to understand the combined effects of chemical reaction and temperature dependent heat source on MHD flow of a couple stress fluid in a vertical wavy porous space with traveling thermal waves. The governing equations of the problem are solved by the perturbation technique using amplitude as a small parameter. The results for flow, heat and mass transfer characteristics have been discussed in detail with the help of graphs.

FORMULATION OF THE PROBLEM

Consider the unsteady, mixed convective heat and mass transfer, MHD flow of a couple stress fluid between two vertical wavy walls embedded in a porous medium. We consider the wavy wall in which the x axis is taken vertically upward, and parallel to the direction of buoyancy, and the y axis is normal to it (Figure 1). A uniform magnetic field is applied normal to the flow direction. The wavy walls are represented by $y=-d+a_1\cos(\lambda x+\vartheta)$ and $y=d+a_1\cos\lambda x$.

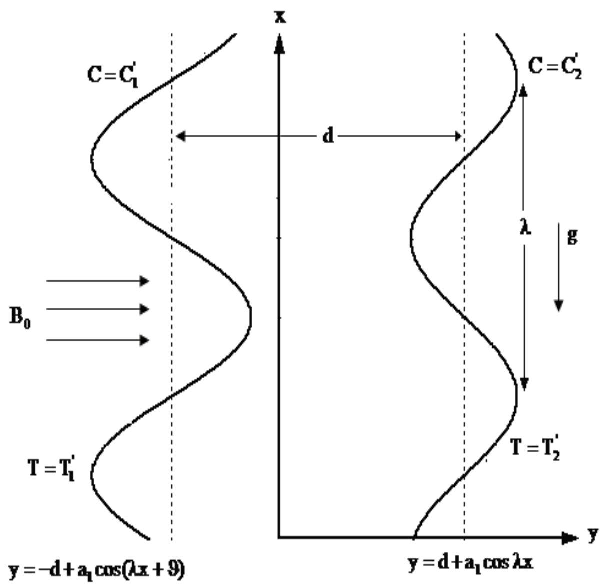

Figure 1. Flow geometry of the problem.

The governing equations for this problem are based on the balance laws of mass, linear momentum and energy modified to account for the presence of the magnetic field, thermal buoyancy and heat generation or absorbing effects. These can be written as:

$$\frac{\partial u}{\partial x}+\frac{\partial v}{\partial y}=0 \tag{1}$$

$$\rho\left(\frac{\partial u}{\partial t}+u\frac{\partial u}{\partial x}+v\frac{\partial u}{\partial y}\right)=-\frac{\partial p}{\partial x}+\mu\nabla^2 u-\eta\nabla^4 u-$$
$$-\frac{\mu\varphi}{k}u-\sigma B_0^2 u+\rho g\beta_t(T-T_1^{'})+\rho g\beta_c(C-C_1^{'}) \tag{2}$$

$$\rho\left(\frac{\partial v}{\partial t}+u\frac{\partial v}{\partial x}+v\frac{\partial v}{\partial y}\right)=-\frac{\partial p}{\partial y}+\mu\nabla^2 v-\eta\nabla^4 v-\frac{\mu\varphi}{k}v \tag{3}$$

$$\rho C_p\left(\frac{\partial T}{\partial t}+u\frac{\partial T}{\partial x}+v\frac{\partial T}{\partial y}\right)=K\nabla^2 T+Q(T-T_1^{'}) \tag{4}$$

$$\left(\frac{\partial C}{\partial t}+u\frac{\partial C}{\partial x}+v\frac{\partial C}{\partial y}\right)=D_m\nabla^2 C-k_1 C \tag{5}$$

where

$$\nabla^2=\left(\frac{\partial^2}{\partial x^2}+\frac{\partial^2}{\partial y^2}\right)$$

The boundary conditions of the problem are:

$$\frac{\partial^2 u}{\partial y^2}=0,\ u=0,\ v=0,\ T=T_1^{'},\ C=C_1^{'},\ \text{at}$$
$$y=-d+a_1\cos(\lambda x+\vartheta) \tag{6}$$

$$\frac{\partial^2 u}{\partial y^2}=0,\ u=0,\ v=0,\ T=T_2^{'},\ C=C_2^{'},\ \text{at}$$
$$y=d+a_1\cos\lambda x \tag{7}$$

where $T_1[1+\varepsilon\cos(\lambda x+\omega t)]=T_1^{'}$, $T_2[1+\varepsilon\cos(\lambda x+\omega t)]=T_2^{'}$, $C_1[1+\varepsilon\cos(\lambda x+\omega t)]=C_1^{'}$, $C_2[1+\varepsilon\cos(\lambda x+\omega t)]=C_2^{'}$, B_0 is the transverse magnetic field, D_m is the coefficient of mass diffusivity, u and v are velocity components, C is the concentration, K is the thermal conductivity of the fluid, k_1 is the first order chemical reaction rate, T is the temperature, p is the pressure, ρ is the density, μ is the dynamic viscosity, ϑ is the phase angle, ν is the kinematic viscosity, φ is the porosity of the medium, k is the permeability of the medium, σ is the coefficient of electric conductivity, η is a constant associated with the couple stress, β_c is the concentration expansion coefficient, β_t is the thermal expansion coefficient, g is the gravitational acceleration, ω is the frequency, T_1 and T_2 are the wall temperatures, C_1 and C_2 are the wall concentrations.

We introduce the non-dimensional variables:

$$(x^*,y^*)=\frac{1}{d}(x,y),\ t^*=\frac{t\overline{U}}{d},\ u^*=\frac{u}{\overline{U}},\ v^*=\frac{v}{\overline{U}},$$
$$p^*=\frac{p}{\rho\overline{U}^2},\ \theta=\frac{T-T_1^{'}}{T_2^{'}-T_1^{'}},\ \phi=\frac{C-C_1^{'}}{C_2^{'}-C_1^{'}} \tag{8}$$

Invoking the above non-dimensional variables, the basic field Eqs. (1)-(7) can be expressed in the non-dimensional form, dropping the asterisks:

$$\frac{\partial u}{\partial x}+\frac{\partial v}{\partial y}=0 \tag{9}$$

$$\frac{\partial u}{\partial t}+u\frac{\partial u}{\partial x}+v\frac{\partial u}{\partial y}=-\frac{\partial p}{\partial x}+\frac{1}{\mathrm{Re}}\left\{\left(\frac{\partial^2 u}{\partial x^2}+\frac{\partial^2 u}{\partial y^2}\right)-\frac{1}{a^2}\left(\frac{\partial^2}{\partial x^2}+\frac{\partial^2}{\partial y^2}\right)^2 u-H^2 u+G_r\theta+G_c\phi\right\} \tag{10}$$

$$\frac{\partial v}{\partial t}+u\frac{\partial v}{\partial x}+v\frac{\partial v}{\partial y}=-\frac{\partial p}{\partial y}+\frac{1}{\mathrm{Re}}\left\{\left(\frac{\partial^2 v}{\partial x^2}+\frac{\partial^2 v}{\partial y^2}\right)-\frac{1}{a^2}\left(\frac{\partial^2}{\partial x^2}+\frac{\partial^2}{\partial y^2}\right)^2 v-\frac{1}{D_a}v\right\} \tag{11}$$

$$\mathrm{Pr}\left(\frac{\partial\theta}{\partial t}+u\frac{\partial\theta}{\partial x}+v\frac{\partial\theta}{\partial y}\right)=\frac{1}{\mathrm{Re}}\left\{\left(\frac{\partial^2\theta}{\partial x^2}+\frac{\partial^2\theta}{\partial y^2}\right)+\alpha_1\theta\right\} \tag{12}$$

$$\left(\frac{\partial\phi}{\partial t}+u\frac{\partial\phi}{\partial x}+v\frac{\partial\phi}{\partial y}\right)=$$
$$=\frac{1}{\mathrm{Re}}\left\{\frac{1}{\mathrm{Sc}}\left(\frac{\partial^2\phi}{\partial x^2}+\frac{\partial^2\phi}{\partial y^2}\right)-\gamma\phi+K_1\right\} \tag{13}$$

The corresponding boundary conditions are:

$$\frac{\partial^2 u}{\partial y^2}=0,\ u=0,\ v=0,\ \theta=0,\ \phi=0\ \text{at}$$
$$y=-1+\varepsilon\cos(\lambda x+\vartheta) \tag{14}$$

$$\frac{\partial^2 u}{\partial y^2}=0,\ u=0,\ v=0,\ \theta=1,\ \phi=1\ \text{at}$$
$$y=-1+\varepsilon\cos\lambda x \tag{15}$$

where $H^2=M^2+1/D_a$, $K_1=-k_1d^2C_1^{'}/((C_2^{'}-C_1^{'})\nu)$, Gr $=d^3\beta_t g(T_2^{'}-T_1^{'})/\nu^2$ is the Grashof number, Gr $=d^3\beta_c g(C_2^{'}-C_1^{'})/\nu^2$ is the local mass Grashof number, Re $=\rho\overline{U}d/\mu$ is the Reynolds number, $M^2=\sigma B_0^2d^2/\mu$ is the Hartmann number, Pr $=\mu C_p/K$ is the Prandtl number, $\nu=\mu/\rho$ is the kinematic viscosity, $\lambda(=\lambda^*)=\lambda d$ is the non dimensional wave number, $\overline{U}$ is the mean velocity, λx is the wall wavinesss parameter, $\varepsilon=a_1/d$ ($\varepsilon \ll 1$) is the non-dimensional amplitude parameter, Sc $=\mu/\rho D_m$ is the Schmidt number, $D_a=k/\varphi d^2$ is the porosity parameter, $a^2=\mu d^2/\eta$ is the couple stress parameter, $\alpha_1=Qd^2/K$ is the heat source/sink parameter and $\gamma=k_1d^2/\nu$ is a chemical reaction parameter.

It has been assumed that the solution consists of a mean part and a perturbed part so that the velocity, temperature and concentration field are [3,9]:

$$
\begin{aligned}
&u(x,y,t)=u_0(y)+\varepsilon u_1(x,y,t);\\
&v(x,y,t)=\varepsilon v_1(x,y,t);\\
&\theta(x,y)=\theta_0(y)+\varepsilon\theta_1(x,y,t);\\
&p(x,y)=p_0(x)+\varepsilon p_1(x,y);\\
&\phi(x,y,t)=\phi_0(y)+\varepsilon\phi_1(x,y,t)
\end{aligned}
\tag{16}
$$

where the perturbed quantities u_1, v_1, θ_1, ϕ_1 and p_1 are small compared to their mean quantities u_0, v_0, θ_0, ϕ_0 and p_0, respectively.

SOLUTION OF THE PROBLEM

In view of the form of Eq. (16), the governing Eqs. (9)-(15) yield:

$$\frac{\mathrm{d}^4u_0}{\mathrm{d}y^4}-a^2\frac{\mathrm{d}^2u_0}{\mathrm{d}y^2}+a^2H^2u_0-a^2(\mathrm{Gr}\theta_0+\mathrm{Gc}\phi_0)=a^2\,\mathrm{Re}\,C^* \tag{17}$$

$$\frac{\mathrm{d}^2\theta_0}{\mathrm{d}y^2}+\alpha_1\theta_0=0 \tag{18}$$

$$\frac{\mathrm{d}^2\phi_0}{\mathrm{d}y^2}-\gamma\mathrm{Sc}\phi_0+K_1\mathrm{Sc}=0 \tag{19}$$

$$\frac{\partial u_1}{\partial x}+\frac{\partial v_1}{\partial y}=0 \tag{20}$$

$$\frac{\partial u_1}{\partial t}+u_0\frac{\partial u_1}{\partial x}+v_1\frac{\partial u_0}{\partial y}=-\frac{\partial p_1}{\partial x}+\frac{1}{\mathrm{Re}}\left\{\left(\frac{\partial^2u_1}{\partial x^2}+\frac{\partial^2u_1}{\partial y^2}\right)-\frac{1}{a^2}\left(\frac{\partial^4u_1}{\partial x^4}+\frac{\partial^4u_1}{\partial y^4}+2\frac{\partial^2u_1}{\partial x^2}\frac{\partial^2u_0}{\partial y^2}\right)-H^2u_1+G_r\theta_1+G_c\phi_1\right\} \tag{21}$$

$$\frac{\partial v_1}{\partial t}+u_0\frac{\partial v_1}{\partial x}=-\frac{\partial p_1}{\partial y}+\frac{1}{\mathrm{Re}}\left\{\left(\frac{\partial^2v_1}{\partial x^2}+\frac{\partial^2v_1}{\partial y^2}\right)-\frac{1}{a^2}\left(\frac{\partial^4v_1}{\partial x^4}+\frac{\partial^4v_1}{\partial y^4}\right)-\frac{1}{D_a}v_1\right\} \tag{22}$$

$$\mathrm{Pr}\left(\frac{\partial\theta_1}{\partial t}+u_0\frac{\partial\theta_1}{\partial x}+v_1\frac{\partial\theta_0}{\partial y}\right)=\frac{1}{\mathrm{Re}}\left\{\left(\frac{\partial^2\theta_1}{\partial x^2}+\frac{\partial^2\theta_1}{\partial y^2}\right)+\alpha_1\theta_1\right\} \tag{23}$$

$$\frac{\partial\phi_1}{\partial t}+u_0\frac{\partial\phi_1}{\partial x}+v_1\frac{\partial\phi_0}{\partial y}=\frac{1}{\mathrm{Re}}\left\{\frac{1}{\mathrm{Sc}}\left(\frac{\partial^2\phi_1}{\partial x^2}+\frac{\partial^2\phi_1}{\partial y^2}\right)-\gamma\phi_1\right\} \tag{24}$$

where

$$C^*=-\frac{\partial p_0}{\partial x}\text{ and }H^2=\left(M^2+\frac{1}{D_a}\right) \tag{25}$$

The boundary conditions become:

$$u_0''=0,\ u_0=0,\ \theta_0=0,\ \phi_0=0,\text{ at }y=-1 \tag{26}$$

$$u_0''=0,\ u_0=0,\ \theta_0=1,\ \phi_0=1\text{ at }y=1 \tag{27}$$

and

$$
\begin{aligned}
&u_1''=-e^{i(\lambda x+\vartheta)}u_0''',\ u_1=-e^{i(\lambda x+\vartheta)}u_0',\ v_1=0,\\
&\theta_1=-e^{i(\lambda x+\vartheta)}\theta_0',\ \phi_1=-e^{i(\lambda x+\vartheta)}\phi_0'\text{ at }y=-1
\end{aligned}
\tag{28}
$$

$$
\begin{aligned}
&u_1''=-e^{i\lambda x}u_0''',\ u_1=-e^{i\lambda x}u_0',\ v_1=0,\ \theta_1=-e^{i\lambda x}\theta_0',\\
&\phi_1=-e^{i\lambda x}\phi_0'\text{ at }y=1
\end{aligned}
\tag{29}
$$

Let us introduce the stream function Ψ defined by:

$$u_1=-\frac{\partial\Psi}{\partial y}\text{ and }v_1=-\frac{\partial\Psi}{\partial x} \tag{30}$$

Using Eq. (30) in Eqs. (21)-(24) and eliminating pressure gradients, we get:

$$
\begin{aligned}
&\psi_xu_{0yy}-(\psi_{xxt}+\psi_{yyt})-u_0(\psi_{xyy}+\psi_{xxx})=\\
&=-\frac{1}{\mathrm{Re}}[\psi_{xxxx}+2\psi_{xxyy}+\psi_{yyyy}]+\\
&+\frac{1}{\mathrm{Re}\,a^2}\begin{bmatrix}\psi_{yyyyyy}+\psi_{yyxxxx}+\psi_{xxyyyy}+\psi_{xxxxxx}+\\+2(\psi_{xxy}u_{0yyy}+\psi_{xxyy}u_{0yy})\end{bmatrix}+\\
&+\frac{1}{\mathrm{Re}}\left[H^2\psi_{yy}+G_r\theta_{1y}+G_c\phi_{1y}+\frac{1}{D_a}\psi_{xx}\right]
\end{aligned}
\tag{31}
$$

$$\mathrm{Pr}[\theta_{1t}+u_0\theta_{1x}+\psi_x\theta_{0y}]=\frac{1}{\mathrm{Re}}\left[\theta_{1xx}+\theta_{1yy}+\alpha\theta_1\right] \tag{32}$$

$$\phi_{1t}+u_0\phi_{1x}+\psi_x\phi_{oy}=\frac{1}{\mathrm{Re}}\left[\frac{1}{Sc}[\phi_{1xx}+\phi_{1yy}]-\gamma\phi_1\right] \tag{33}$$

The boundary conditions (28) and (29) become:

$$
\begin{aligned}
&\Psi_{yyy}=e^{i(\lambda x+\vartheta)}u_0''',\ \Psi_y=e^{i(\lambda x+\vartheta)}u_0',\ \Psi_x=0,\\
&\theta_1=-e^{i(\lambda x+\vartheta)}\theta_0',\ \phi_1=-e^{i(\lambda x+\vartheta)}\phi_0'\text{ at }y=-1
\end{aligned}
\tag{34}
$$

$$
\begin{aligned}
&\Psi_{yyy}=e^{i\lambda x}u_0''',\ \Psi_y=e^{i\lambda x}u_0',\ \Psi_x=0,\\
&\theta_1=-e^{i\lambda x}\theta_0',\ \phi_1=-e^{i\lambda x}\phi_0'\text{ at }y=1
\end{aligned}
\tag{35}
$$

We assume that the solution in the form:

$$\Psi(x,y,t)=e^{i(\lambda x+\omega t)}\Psi_1(y) \tag{36}$$

$$\theta_1(x,y,t)=e^{i(\lambda x+\omega t)}\overline{\theta}_1(y) \tag{37}$$

$$\phi(x,y,t) = e^{i(\lambda x+\omega t)}\bar{\phi}_1(y) \tag{38}$$

Using Eqs. (36)-(38), Eqs. (31)-(33) become:

$$i\lambda\psi_1 u_{0yy} + (i\lambda^2\omega\psi_1 - i\omega\psi_{1yy}) - u_0(i\lambda\psi_{1yy} - i\lambda^3\psi_1) = -\frac{1}{\mathrm{Re}}[\lambda^4\psi_1 - 2\lambda^2\psi_{1yy} + \psi_{1yyyy}] + \frac{1}{\mathrm{Re}\,a^2}\times$$
$$\times\left[\psi_{1yyyyyy} + \lambda^4\psi_{1yy} - \lambda^2\psi_{1yyyy} - \lambda^6\psi_1 - 2(\lambda^2\psi_{1y}u_{0yyy} + \lambda^2\psi_{1yy}u_{0yy})\right] + \frac{1}{\mathrm{Re}}\left[H^2\psi_{1yy} + G_r\bar{\theta}_{1y} + G_c\bar{\phi}_{1y} + \frac{\lambda^2}{D_a}\psi_1\right] \tag{39}$$

$$\Pr[i\omega\bar{\theta}_1 + i\lambda u_0\bar{\theta}_1 + i\lambda\bar{\psi}\theta_{0y}] = \frac{1}{\mathrm{Re}}\left[-\lambda^2\bar{\theta}_1 + \bar{\theta}_{1yy} + \alpha_1\bar{\theta}_1\right] \tag{40}$$

$$i\omega\bar{\phi}_1 + i\lambda u_0\bar{\phi}_1 + i\lambda\bar{\psi}_1\phi_{oy} = \frac{1}{\mathrm{Re}}\left[\frac{1}{\mathrm{Sc}}(-\lambda^2\bar{\phi}_1 + \bar{\phi}_{1yy}) - \gamma\bar{\phi}_1\right] \tag{41}$$

with the boundary conditions:

$$\Psi_1''' = e^{i(\vartheta-\omega t)}u_0''',\ \Psi_1' = e^{i(\vartheta-\omega t)}u_0',\ \Psi_1 = 0,$$
$$\bar{\theta}_1 = -e^{i(\vartheta-\omega t)}\theta_0',\ \bar{\phi}_1 = -e^{i(\vartheta-\omega t)}\phi_0' \text{ at } y = -1 \tag{42}$$

$$\Psi_1''' = e^{-i\omega t}u_0''',\ \Psi_1' = e^{-i\omega t}u_0',\ \Psi_1 = 0,\ \bar{\theta}_1 = -e^{-i\omega t}\theta_0',$$
$$\bar{\phi}_1 = -e^{-i\omega t}\phi_0' \text{ at } y = 1 \tag{43}$$

For small values of λ, we can expand Ψ_1, $\bar{\theta}_1$ and $\bar{\phi}_1$ in terms of λ so that:

$$\Psi_1(\lambda,y) = \sum_{r=0}^{\infty}\lambda^r\Psi_{1r},\ \bar{\theta}_1(\lambda,y) = \sum_{r=0}^{\infty}\lambda^r\bar{\theta}_{1r},$$
$$\bar{\phi}_1(\lambda,y) = \sum_{r=0}^{\infty}\lambda^r\bar{\phi}_{1r} \tag{44}$$

Substituting Eq. (44) into Eqs. (39)-(43), we get the following set of ordinary differential equations and the boundary conditions:

$$\Psi_{10}^{vi} - a^2\Psi_{10}^{iv} + a^2(H^2 + i\,\mathrm{Re}\,\omega)\Psi_{10}'' +$$
$$+a^2\mathrm{Gr}\bar{\theta}_{10}' + a^2\mathrm{Gc}\bar{\phi}_{10}' = 0 \tag{45}$$

$$\bar{\theta}_{10}'' + (\alpha_1 - i\omega\mathrm{Re}\Pr)\bar{\theta}_{10} = 0 \tag{46}$$

$$\bar{\phi}_{10}'' - \mathrm{Sc}(\gamma + i\omega\mathrm{Re})\bar{\phi}_{10} = 0 \tag{47}$$

With boundary conditions:

$$\Psi_{10}''' = e^{i(\vartheta-\omega t)}u_0''',\ \Psi_{10}' = e^{-i\omega t}u_0',\ \Psi_{10} = 0,$$
$$\bar{\theta}_{10} = -e^{i(\vartheta-\omega t)}\theta_0',\ \bar{\phi}_{10} = -e^{i(\vartheta-\omega t)}\phi_0' \text{ at } y = -1 \tag{48}$$

$$\Psi_{10}''' = e^{-i\omega t}u_0''',\ \Psi_{10}' = e^{-i\omega t}u_0',\ \Psi_{10} = 0,\ \bar{\theta}_{10} = -e^{-i\omega t}\theta_0',$$
$$\bar{\phi}_{10} = -e^{-i\omega t}\phi_0' \text{ at } y = 1 \tag{49}$$

Zeroth-order solution. The solution of Eqs.(17)-(19) subject to the boundary conditions (26)-(27) are:

$$\mathrm{u}_0(y) = A_2\cosh\beta_2 y + B_2\sinh\beta_2 y + C_2\cosh\beta_3 y +$$
$$+D_2\sinh\beta_3 y + T_6\cos\alpha y + T_7\sin\alpha y + T_8\cosh\beta_1 y + \tag{50}$$
$$+T_9\sinh\beta_1 y + T_{10}$$

$$\theta_0(y) = A\cos\alpha y + B\sin\alpha y \tag{51}$$

$$\phi_0(y) = A_1\cosh\beta_1 y + B_1\sinh\beta_1 y + \frac{K_1\mathrm{Sc}}{\beta_1^2} \tag{52}$$

where:

$$\beta_1 = \sqrt{\gamma\mathrm{Sc}}\ ;\ H = \sqrt{M^2 + \frac{1}{D_a}}\ ;\ \beta_2 = \sqrt{\frac{a^2 + a\sqrt{a^2 - 4H^2}}{2}}\ ;$$
$$\beta_3 = \sqrt{\frac{a^2 - a\sqrt{a^2 - 4H^2}}{2}}$$

First order solution. The solutions of Eqs. (45)-(47), subjected to the conditions (48) and (49) are:

$$\Psi_{10} = A_5 + B_5 y + C_5\cosh\beta_7 y + D_5\sinh\beta_7 y +$$
$$+E_5\cosh\beta_8 y + F_5\sinh\beta_8 y + T_{15}\sin\beta_5 y + \tag{53}$$
$$+T_{16}\cos\beta_5 y + T_{17}\sinh\beta_4 y + T_{18}\cosh\beta_4 y$$

$$\bar{\theta}_{10} = A_4\cos\beta_5 y + B_4\sin\beta_5 y \tag{54}$$

$$\bar{\phi}_{10} = A_3\cosh\beta_4 y + B_3\sinh\beta_4 y \tag{55}$$

where:

$$\beta_4 = \sqrt{\mathrm{Sc}(\gamma + i\omega\mathrm{Re})}\ ;\ \beta_5 = \sqrt{\alpha_1 + i\omega\mathrm{Re}\Pr}\ ;$$
$$\beta_6 = \sqrt{a^2(i\omega\mathrm{Re} + H^2)}\ ;\ \beta_7 = \sqrt{\frac{a^2 + \sqrt{a^4 - 4\beta_6}}{2}}\ ;$$
$$\beta_8 = \sqrt{\frac{a^2 - \sqrt{a^4 - 4\beta_6}}{2}}$$

The shear stress at any point in the fluid is given by:

$$\bar{\tau}_{xy} = \mu\left(\frac{\partial u}{\partial y} + \frac{\partial v}{\partial x}\right) \tag{56}$$

In nondimensionless form:

$$\tau = \frac{d^2}{\rho v^2}\bar{\tau}_{xy} = \frac{\partial u}{\partial y} + \frac{\partial v}{\partial x} \tag{57}$$

At the wavy walls $y = -1 + \varepsilon\cos(\lambda x + \vartheta)$ and $y = 1 + \varepsilon\cos\lambda x$, the skin friction τ_{xy} becomes:

$$\tau_1 = \tau_1^0 - \varepsilon\,\mathrm{R.}P \text{ of}$$
$$[e^{i(\lambda x+\vartheta)}\mathrm{u}_0''(-1) + e^{i(\lambda x+\omega t)}\Psi_{10}''(-1)] \tag{58}$$

$$\tau_2 = \tau_2^0 - \varepsilon \mathrm{R.}P \text{ of } [e^{i\lambda x} u_0''(1) + e^{i(\lambda x+\omega t)} \Psi_{10}''(1)] \quad (59)$$

respectively, where:

$$\tau_1^0 = -u_0'(-1)\,;\ \tau_2^0 = -u_0'(1) \quad (60)$$

The heat transfer coefficient, characterized by Nusselt number (Nu) on the tube boundary is:

$$h^* = -K\frac{\partial T}{\partial y} \quad (61)$$

In dimensionless form it becomes:

$$h^* = -K\left(\frac{T_2' - T_1'}{d}\right)\left[\begin{array}{l}\theta_0''(y) + \mathrm{R.}P\ of \\ \left\{\varepsilon\,[e^{i(\lambda x+\omega t)} \bar{\theta}_{10}'(y)]\right\}\end{array}\right] \quad (62)$$

At the wavy walls $y = -1 + \varepsilon\cos(\lambda x + \vartheta)$ and $y = 1 + \varepsilon\cos\lambda x$, the Nusselt number becomes:

$$\mathrm{Nu}_1 = \mathrm{Nu}_1^0 + \varepsilon R.P \text{ of } \left\{[e^{i(\lambda x+\vartheta)} \theta_0''(-1) + e^{i(\lambda x+\omega t)} \bar{\theta}_{10}'(-1)]\right\} \quad (63)$$

$$\mathrm{Nu}_2 = \mathrm{Nu}_2^0 + \varepsilon R.P \text{ of } \left\{[e^{i\lambda x} \theta_0''(1) + e^{i(\lambda x+\omega t)} \bar{\theta}_{10}'(1)]\right\} \quad (64)$$

respectively, where:

$$\mathrm{Nu}_1^0 = \theta_0'(-1)\,;\ \mathrm{Nu}_2^0 = \theta_0'(1) \quad (65)$$

The dimensionless mass transfer number corresponding to the Nusselt number is the Sherwood number, written as

$$Sh = \frac{\partial\phi}{\partial y} \quad (66)$$

At the wavy walls $y = -1 + \varepsilon\cos(\lambda x + \vartheta)$ and $y = 1 + \varepsilon\cos\lambda x$, Sherwood number becomes:

$$\mathrm{Sh}_1 = \mathrm{Sh}_1^0 + \varepsilon R.P \text{ of } \left\{[e^{i(\lambda x+\vartheta)} \phi_0''(-1) + e^{i(\lambda x+\omega t)} \bar{\phi}_{10}'(-1)]\right\} \quad (67)$$

$$\mathrm{Sh}_2 = \mathrm{Sh}_2^0 + \varepsilon R.P \text{ of} [e^{i\lambda x} \phi_0''(1) + e^{i(\lambda x+\omega t)} \phi_1'(1)] \quad (68)$$

respectively, where:

$$\mathrm{Sh}_1^0 = \phi_0'(-1)\,;\ \mathrm{Sh}_2^0 = \phi_0'(1) \quad (69)$$

and $R.P$ denotes the real part.

RESULTS AND DISCUSSIONS

In order to get a clear insight of the physical problem, the heat and mass transfer characteristics of the fluid flow have been discussed by assigning numerical values to couple stress parameter (a), Hartmann number (M), permeability parameter (D_a), Prandtl number (Pr), Grashof number (Gr), local Grashof number (G_c), chemical reaction parameter (γ), heat source parameter (α_1) and Schmidt number (Sc). Figure 2 has been plotted in order to see the effects of M, D_a, (α_1, a, γ and Gr on velocity distribution. Figure 2a shows that the velocity profiles decrease with an increase of the strength of the magnetic field. As M increases, the Lorentz force, which opposes the flow, also increases and leads to enhanced deceleration of the flow. The effect of the permeability parameter on u is illustrated in Figure 2b. As anticipated, the increase of permeability parameter reduces the drag force and hence causes the flow velocity to increase. Figure 2c is sketched to understand the influence of heat source parameter (α_1) on velocity distribution. It shows that the velocity increases significantly with increasing α_1. A similar effect to that is shown in Figure 2d, if α_1 is replaced by couple stress parameter (a). The influence of chemical reaction parameter (γ) on u is shown in Figure 2e. It shows that increasing γ lead to suppress the velocity. The effect of Gr on velocity is shown in Figure 2f. It depicts that the velocity enhances with an increase of Gr. This is because increasing the buoyancy ratio tends to accelerate the fluid flow.

The cross velocity (v) is plotted in Figure 3 for different values of ϑ, α_1 and Sc. Figure 3a depicts how cross velocity decreases with an increase of ϑ. Figure 3b displays that in the presence of α_1, the fluid velocity decreases. In Figure 3c, increasing Sc velocity profiles are decreased steadily near the walls, while in center of the channel u is an increasing function of y. The behavior of temperature profiles for different values of $\alpha_1$is shown in Figure 4. It is well known that the heat generation (*i.e.*, $\alpha_1 > 0$) causes the fluid temperature to increase, which has a tendency to increase the thermal buoyancy effects. On the other hand, heat absorption (*i.e.*, $\alpha_1 < 0$) produces opposite effect.

The effect of γ and Sc on concentration distribution is analyzed through Figure 5. To be realistic, the values of Schmidt number are chosen to be 0.5, 0.6, 0.78, 1 and 2 (which corresponds to hydrogen gas, water vapor, ammonia, carbon dioxide at 25 °C, and ethyl benzene in air, respectively). Figure 5a indicates that ϕ decreases significantly with both γ and y. A similar result can be observed in Figure 5b, if γ is replaced by Sc. The variation in skin friction (τ) for various values of γ and a is displayed in Figure 6. Figure 6a displays skin friction decreases with increasing

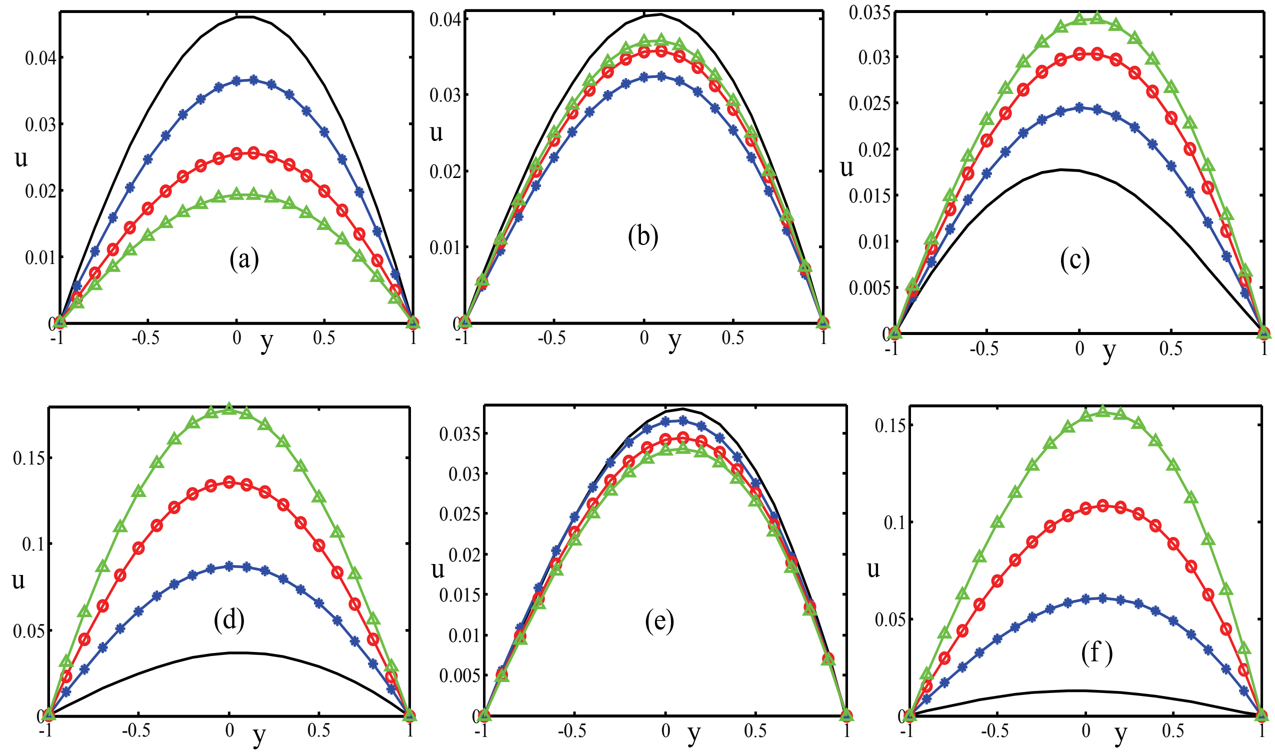

Figure 2. Velocity distribution; $G_c = 1$, $Re = 1$, $K_1 = 1$, $t = 1$, $\omega = 1$, $\varepsilon = 0.001$, $\vartheta = 0$, $C^* = 1$, $Pr = 0.71$, $\lambda x = 0.02$; a) (–) $M = 0$, (✳) $M = 2$, (○) $M = 4$, (△) $M = 6$, $D_a = 0.5$, $\gamma = 0.5$, $Gr = 1$, $Sc = 0.5$, $a = 0.2$, $\alpha_1 = 0.5$; b) (–) $D_a = \infty$, (✳) $D_a = 0.1$, (○) $D_a = 0.2$, (△) $D_a = 0.3$, $M = 2$, $Gr = 1$, $\gamma = 0.5$, $a = 0.2$, $Sc = 0.5$; c) (–) $\alpha_1 = 0$, (✳) $\alpha_1 = 0.1$, (○) $\alpha_1 = 0.2$, (△) $\alpha_1 = 0.3$, $D_a = 0.5$, $Gr = 1$, $a = 0.2$, $M = 2$, $Sc = 0.5$; d) (–) $a = 0.2$, (✳) $a = 0.4$, (○) $a = 0.6$, (△) $a = 0.8$, $D_a = 0.5$, $Gr = 1$, $M = 2$, $\gamma = 0.5$, $Sc = 0.5$; e) (–) $\gamma = -0.5$, (✳) $\gamma = 0.5$, (○) $\gamma = 5$, (△) $\gamma = 15$, $D_a = 0.5$, $M = 2$, $Gr = 1$, $a = 0.2$, $\gamma = 0.5$, $Sc = 0.5$; f) (–) $Gr = 0$, (✳) $Gr = 2$, (○) $Gr = 4$, (△) $Gr = 6$, $D_a = 0.5$, $M = 2$, $\gamma = 0.5$, $Sc = 0.5$, $a = 0.2$.

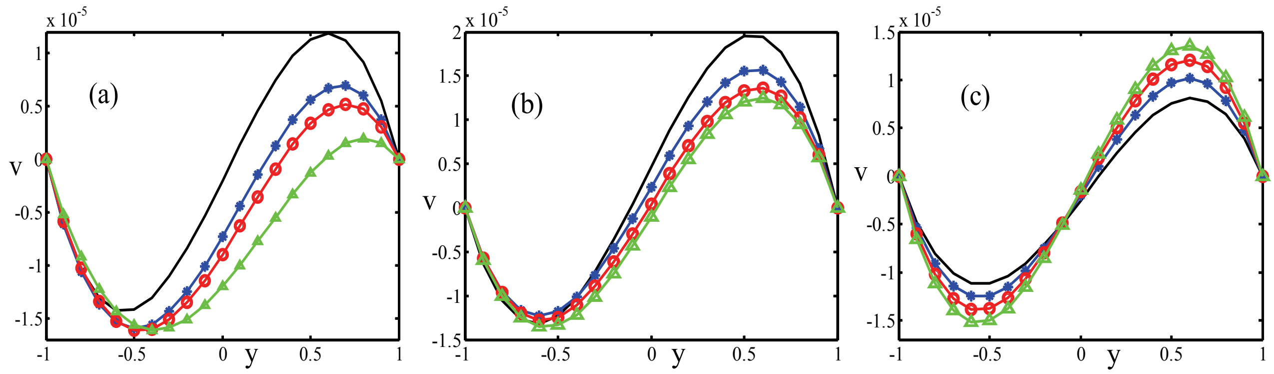

Figure 3. Cross velocity distribution; $G_c = 5$, $Gr = 5$, $C^* = 1$, $t = 1$, $\omega = 1$, $D_a = 0.5$, $\varepsilon = 0.001$, $M = 2$, $\gamma = 0.5$, $K_1 = 1$, $a = 0.2$, $\lambda x = 0.02$, $Pr = 0.71$; a) (–) $\vartheta = 0$, (✳) $\vartheta = \pi/8$, (○) $\vartheta = \pi/6$, (△) $\vartheta = \pi/4$, $\alpha_1 = 0.5$, $Sc = 0.5$; b) (–)$\alpha_1 = 0.1$, (✳) $\alpha_1 = 0.2$, (○) $\alpha_1 = 0.3$, (△) $\alpha_1 = 0.4$, $Sc = 0.5$, $\vartheta = 0$; c) (–) $Sc = 0$, (✳) $Sc = 0.1$, (○) $Sc = 0.2$, (△) $Sc = 0.3$, $\alpha_1 = 0.5$, $\vartheta = 0$.

γ at both the walls. Also, it may be noted that skin friction enhances with an increase of G_c while it decreases with increasing γ at the wall $y = -1$ whereas skin friction decreases with increasing γ as well as G_c at the other wall $y = 1$. The reverse trend can be seen for the case of increasing the value of couple stress parameter, as shown in Figure 6b.

The effects of various values of Pron Nusselt number distribution have been shown in Figure 7. Figure 7a illustrates that Nusselt number enhances with increase in value of Pr and α_1 at the wall $y = 1$ but it is reversed at the other wall $y = -1$. From Figure 7b, we may note that Nu decreases with increasing ϑ at both the walls. Further we observe from the same figure that Nu increases with an increase of α at the wall $y = -1$

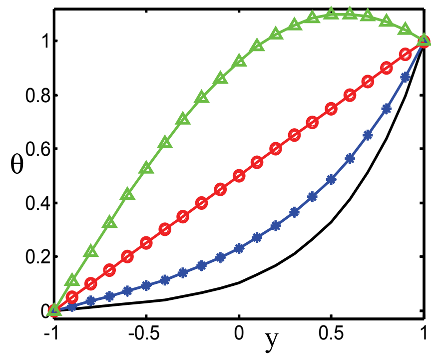

Figure 4. Temperature distribution; Pr = 0.71, t = 1, Re = 1, ω = 1, ε = 0.001, ϑ = 0, λx = 0.02; (–) α_1=-5, (✳) α_1 = -3, (○) α_1 = 0, (△) α_1 = 1.

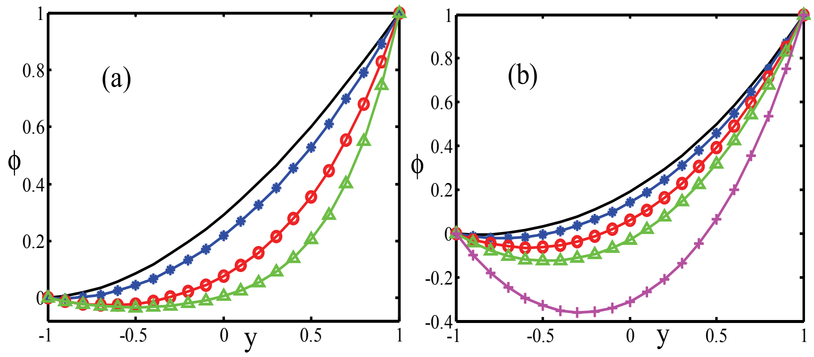

Figure 5. Concentration distribution; Re = 1, K_1 = -1, t = 1, ω = 1, ε = 0.001, ϑ = 0, λx = 0.02; a) (–) γ =-0.5, (✳) γ =0.5, (○) γ =1 .5, (△) γ = 3, Sc = 0.5; b) (–) Sc = 0.5, (✳) Sc = 0.6, (○) Sc = 0.78, (△) Sc = 1, (+) Sc =2, γ = 1.

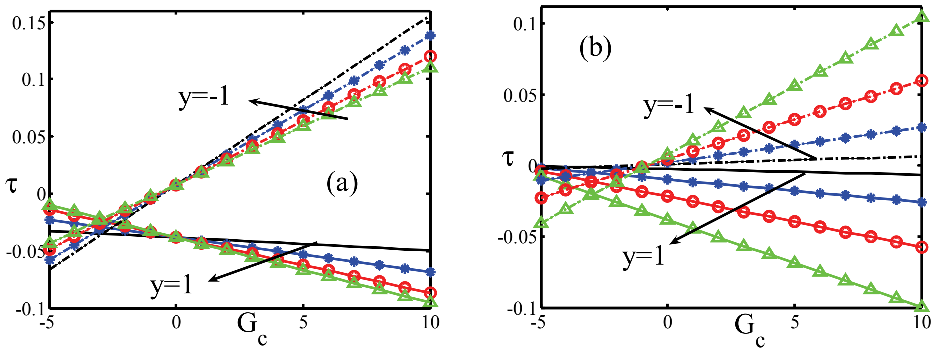

Figure 6. Skin friction distribution; Gr = 5, Re = 1, C = 1, t = 1, ω = 1, M = 2, D_a = 0.5, ε = 0.001, α_1 = 6, ϑ = π/2, K_1 = 1, Pr = 0.71, λx = 0.02; a) (–) γ = 0.1, (✳) γ = 0.2, (○) γ = 0.3, (△) γ = 0.4, a = 0.2; b) (–) a = 0.05, (✳) a = 0.1, (○) a = 0.15, (△) a = 0.2, γ = 0.5.*

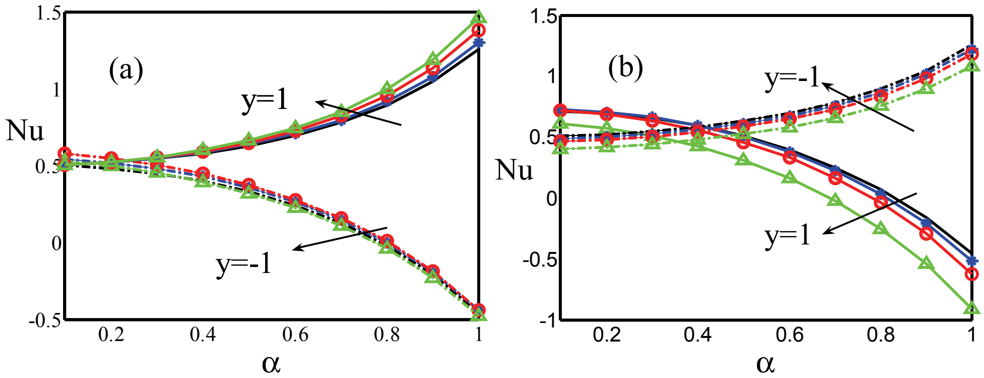

Figure 7. Nusselt number distribution; Re = 1, t = 1, ω =1, ε = 0.3, λx = 0.02; a) (–) Pr = 1, (✳) Pr = 3, (○) Pr = 5, (△) Pr = 7, ϑ = 0; b) (–) ϑ = 0, (✳) ϑ = π/8, (○) ϑ = π/4, (△) ϑ = π/2, Pr = 0.71.

but the opposite effect can be noticed at the other wall. Figure 8 illustrates the effect of Sc and γ on Sherwood number distribution at the channel walls. It reveals that an increase in γ leads to increase in the rate of mass transfer.

CONCLUSIONS

The problem of MHD mixed convective heat and mass transfer flow of a couple-stress fluid in a vertical wavy porous space in the presence of chemical reaction and temperature dependent heat source with travelling thermal waves has been studied. Such flow analysis plays an important role in many engineering applications, such as oil recovery, food processing, paper making and slurry transporting. The dimensionless governing equations are perturbed into: mean (zeroth-order) part and a perturbed part, using amplitude as a small parameter. Analytical solutions for velocity, temperature and concentration field have been obtained. The heat and mass transfer characteristics on fluid flow are discussed with the help of graphs. The main findings are summarized as follows.

- The velocity of the fluid increases with an increase of D_a, α_1 and a while it decreases with increasing M and γ.
- Increasing α_1 leads to enhance fluid temperature.
- The parameters γ and Sc lead to decrease the fluid concentration.
- Increasing γ lead to decrease skin friction at both the walls. Increasing G_c lead to increase τ at the wall $y = -1$ but the opposite trend can be seen at the other wall.
- Sherwood number decreases with an increase of Sc at the wall $y = -1$ while it increases at the other wall.

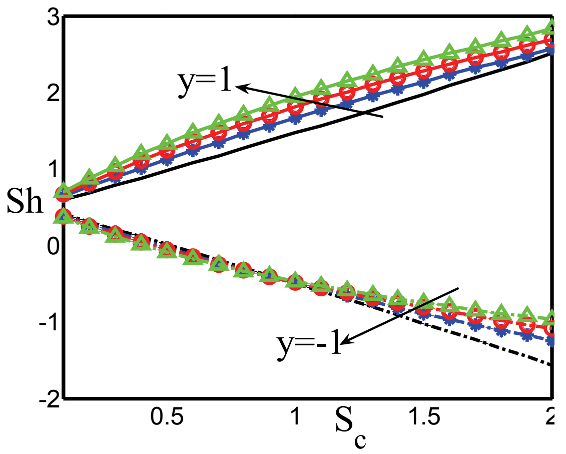

Figure 8. Sherwood number distribution, $Re = 1$, $t = 1$, $\omega = 1$, $\vartheta = 0$, $\varepsilon = 0.01$, $\alpha_1 = 0.5$, $K_1 = 1$, $Pr = 0.71$, $\lambda x = 0.02$; (–) $\gamma = -0.1$, (✳) $\gamma = 0.5$, (○) $\gamma = 1$, (△) $\gamma = 1.5$.

Acknowledgement

Authors acknowledge the financial support from Department of Science and Technology, Govt. of India, under the project number SR/S4.MS:674/10.

Nomenclature

a - Couple stress parameter
B_0 - Magnetic field
C_1, C_2 - Wall concentrations
C - Concentration of the fluid
D_a - Porosity parameter
D_m - Coefficient of mass diffusivity
g - Gravitational acceleration
Gr - Grashof number
G_c - Local mass Grashof number
K - Thermal conductivity of the fluid
k_1 - First order chemical reaction rate
k - Permeability of the medium
M - Hartmann number
p - Pressure
Pr - Prandtl number
Re - Reynolds number
Sc - Schmidt number
T - Temperature of the fluid
T_1, T_2 - Wall temperatures
u, v - Velocity components
$\overline{U}$ - Mean velocity

Greek symbols

α_1 - Heat source/sink parameter
β_c - Concentration expansion coefficient
β_t - Thermal expansion coefficient
γ - Chemical reaction parameter
μ - Dynamic viscosity
ρ - Density
ϑ - Phase angle
ν - Kinematic viscosity
φ - Porosity of the medium
σ - Coefficient of electric conductivity
η - A constant associated with the couple stress
ω - Frequency
λ - The nondimensional wave number
λx - Wall wavinesss parameter
ε - Nondimensional amplitude parameter

Subscripts

0 - Mean quantities
1 - Perturbed quantities

REFERENCES

[1] L.N. Tao, ASME J. Heat Trans. **82** (1960) 233-238
[2] W. Aung, G. Worku, ASME J. Heat Trans.**108** (1986) 485-488
[3] K. Vajravelu, Int. J. Engg. Sci. **27** (1989) 289- 300
[4] A. Barletta, Int. J. Heat Mass Trans. **41** (1998) 3873-3885
[5] A.J. Chamkha, J. Fluids, Engg.-ASME. **22** (2000)117-124
[6] J.H. Jang, W.M. Yan, Int. J. Heat Mass Trans. **47** (2004) 419-428
[7] N.T. Eldabe, M.F. El-Sayed, A.Y. Ghaly, H.M. Sayed, Arch. Appl. Mech. **78** (2008) 599-624
[8] S. Srinivas, R. Muthuraj, Commun. Nonlinear Sci. Numer. Simul. **15** (2010) 2098-2108
[9] R. Muthuraj, S. Srinivas, Comput. Math. Appl. **59** (2010) 3516-3528
[10] L. Zheng, L. Wang, X. Zhang, Commun. Nonlinear Sci. Numer. Simul. **16**(2011) 731-740
[11] J. Prathap Kumar, J.C. Umavathi, B.M. Biradar, Int. J. Non-Linear Mech. **46** (2011) 278-285
[12] V.K. Stokes, Phys. Fluids **9** (1966) 1709-1715
[13] E.F. Elshehawey, Kh.S. Mekheimer, J. Phys., D **27** (1994) 1163-1170
[14] Sunil, R.C. Sharma, M. Pal, J. Porous Media **5** (2002) 149-158

[15] S.N. Gaikwad, M.S. Malashetty, K. Ramaprasad, Int. J. Non linear Mech. **42** (2007) 903-913

[16] N. Ali, T. Hayat, M. Sajid, J. Biorheology **44** (2007) 125-138

[17] Kh.S. Mekheimer, Phys. Lett., A **372** (2008) 4271-4278

[18] A. M. Sobh, Turkish J. Eng. Env. Sci. **32** (2008) 117-123

[19] D. Srinivasacharya, N. Srinivasacharyulu, O. Odelu, Int. Commun. Heat Mass Trans. **36** (2009) 180-185

[20] S.K. Pandey, Meccanica, DOI: 10.1007/s11012-010-9387-8

[21] S.Nadeem, S. Akram, Arch. Appl. Mech. **81** (2011) 97-109

[22] R. Muthucumarswamy, P. Ganesan, Int. J. Therm. Sci. **41** (2002) 475-479

[23] K.V. Prasad, S. Abel, P.S. Datti, Int. J. Non-Linear Mech. **38** (2003) 651-657

[24] P.M. Patil, P.S. Kulkarni, Int. J. Thermal Sci. **47** (2008) 1043-1054

[25] T. Hayat, Z. Abbas, M. Sajid, Phys. Lett., A **372** (2008) 2400-2408

[26] D. Pal, B. Talukdar, Commun. Nonlinear Sci. Numer. Simul. **15** (2010)1813-1830

[27] T. Hayat, M. Mustafa, S. Asghar, Nonlinear Anal. Real World Appl. **11** (2010) 3186-3197

[28] S. Srinivas, R. Muthuraj, Math. Comput. Model. **54** (2011) 1213-1227.

R. MUTHURAJ[1]
S. SRINIVAS[2]
D. LOURDU IMMACULATE[3]

[1]Department of Mathematics, P.S.N.A. College of Eng. &Tech., Dindigul, India
[2]Fluid Dynamics Division, VIT University, Vellore, India
[3]Department of School education, Othakadi, Madurai, Government of Tamilnadu, India

NAUČNI RAD

KOMBINOVANI UTICAJI HEMIJSKE REAKCIJE I TOPLOTNOG IZVORA PROMENLJIVE TEMPERATURE NA MHD PRELAZNOG KONVEKTIVNOG STRUJANJA FLUIDA SA NAPONSKIM SPREGOM KROZ VERTIKALNI TALASASTI POROZNI PROCTOR SA PUTUJUĆIM TOPLOTNIM TALASIMA

Razvijen je matematički model u cilju istraživanja efekta hemijske reakcije na MHD prelaznog konvektivnog prenosa toplote I mase strujanjem fluida sa naponskim spregom kroz vertikalni porozni proctor u prisustvu toplotnog izvora promenljive temperaturesa putujućim toplotnim talasima. Pretpostavljeno je da se bezdimenzionalne jednačine sastoje iz dva dela: srednji deo koji odgovara potpuno razvijenom toku i malog poremećenog dela, koristeći amplitude kao mali parameter. Analitička rešenja drugog dela is nađena korišćenjem aproksimacijom dugih talasa. Dobijeni su izrazi za resenja nultog i prvog reda, a rezultati toplotnih i maseno-prenosnih karakteristika su prikazani grafički za različite vrednosti parametara uključenih u problem. Zapaženo je da se brzina fluida povećava sa povećanjem parametra naposnkog sprega, dok povećanje parametra hemijske reakcije vodi smanjenju brzine fluida. Poprečna brzina se smanjuje sa povećanjem faznog ugla. Povećanje parametra hemijske reakcije i Šmitovog broja vodi smanjenju koncentracije fluida. Hidrodinamički slučaj za neporozni prostor u odsustvu toplotnog izvora promenljive temperature za njutnovski fluid se može smatrati graničnim slučajem sprovedene analize uzimajući da je $H, \alpha_1 \rightarrow \infty$, $D_a \rightarrow \infty$ and $a \rightarrow \infty$.

Ključne reči: prelazna konvekcija, talasasti zidovi, porozni prostor, fluid sa naponskim spregom, hemijska reakcija.